Primary epithelial-myoepithelial carcinoma of the lung: A case report demonstrating high-grade transformation-like changes

SHOGO TAJIMA[1], MICHIHIKO AKI[2], KIYOSHIGE YAJIMA[3], TSUYOSHI TAKAHASHI[3], HIROSHI NEYATANI[3] and KENJI KODA[4]

[1]Department of Pathology, Shizuoka Saiseikai General Hospital, Shizuoka, Shizuoka 422-8021; [2]Department of Cell Biology and Anatomy, Hamamatsu University School of Medicine, Hamamatsu, Shizuoka 431-3192; Departments of [3]Chest Surgery and [4]Pathology, Fujieda Municipal General Hospital, Fujieda, Shizuoka 426-0077, Japan

Received August 3, 2014; Accepted March 19, 2015

DOI: 10.3892/ol.2015.3169

Abstract. Primary salivary gland-type tumors of the lung are rare; among them, epithelial-myoepithelial carcinomas (EMC) represent a minor histological subtype. The present case documents an EMC that occluded the B8 segment of the left lung in a 72-year-old woman. Macroscopically, the tumor was well-demarcated; however, microscopic examination demonstrated that it had infiltrated the lung parenchyma. The majority of the tumor mass was composed of a myoepithelial overgrowth in conjunction with conventional bilayered ductal structures comprising epithelial and myoepithelial cells. At the advancing edge of the tumor, the myoepithelial overgrowth was observed to be gradually transitioning to a higher-grade component, which demonstrated venous invasion. The Ki-67 labeling index was reduced compared with high-grade transformation (HGT) of salivary gland EMC; p53 was sparsely observed on immunostaining. However, cyclin D1, which is reported to be overexpressed in certain subtypes of salivary gland carcinomas with HGT, was overexpressed in the higher-grade component of the tumor, indicating a potential HGT initiation. The surgical margin was tumor free, and no recurrence has been observed for 4 months. A thorough follow-up is required considering the HGT-like changes and venous invasion of the tumor. Additional studies are required to elucidate the characteristics of pulmonary EMC, with an emphasis on detecting HGT or HGT-like changes.

Introduction

Primary salivary gland-type tumors of the lung account for ~0.1-1% of all primary lung carcinomas; among them, the most frequently observed histological subtype is mucoepidermoid carcinoma, followed by adenoid cystic carcinoma (1,2). Epithelial-myoepithelial carcinoma (EMC) is less common and accounts for approximately 4 and 8% of the primary salivary gland-type tumors in Korea and China, respectively (1,2). There have been ~50 cases of pulmonary EMC reported to date (3).

The presence of EMC in the salivary gland was first described by Donath *et al* in 1972 (4). EMCs have now been demonstrated to account for 1.0% of all salivary gland tumors (5). Despite its predilection for the parotid gland, EMC also occurs less frequently in other locations, including the minor salivary glands or seromucous gland sites, such as the upper and lower respiratory tract (5). EMC of the salivary gland is considered to derive from the intercalated duct (6). It is speculated that the tumor originates from the ductal structure of the bronchial gland, which is a counterpart of the lungs (7). Each tumor nest presents with a characteristic morphology comprised of a biphasic pattern with an inner layer of epithelial cells and an outer layer of myoepithelial cells. The characteristics of its counterpart in the lung remain to be elucidated due to the limited number of cases. A number of pathologists have proposed the term pulmonary epithelial-myoepithelial tumor to describe this type of tumor, which has unproven malignant potential (8); however, there have been at least 3 reported cases of high-grade pulmonary EMC that presented with metastasis in the regional lymph nodes (9), bone (2) and chest wall (3).

The sequential development of high-grade malignancies inside pre-existing tumors has recently been defined as 'high-grade transformation' (HGT). The term 'dedifferentiation' once included HGT; however, it is now only applied in situations in which a high-grade neoplasm that has progressed from a low-grade neoplasm loses the histological characteristics of its original lineage (10). Salivary EMCs and numerous other histological subtypes have been reported to undergo HGT (10). Although EMC is generally considered to be a low-grade malignancy with good clinical prognosis (5,11), a number of studies have revealed that EMC with HGT is exceptionally aggressive, and exhibits poor prognosis with a high rate of distant metastasis (12). Although >20 cases of EMC with HGT concentrated in the salivary glands have previously been reported (13), to the best of our knowledge, pulmonary EMCs with HGT have yet to be documented. In the present case report, a case of EMC is presented that demonstrates progression of the

Correspondence to: Dr Shogo Tajima, Department of Pathology, Shizuoka Saiseikai General Hospital, 1-1-1 Oshika, Suruga-ku, Shizuoka, Shizuoka 422-8021, Japan
E-mail: stajima-tky@umin.ac.jp

Key words: epithelial-myoepithelial carcinoma, high-grade transformation, lung, cyclin D1

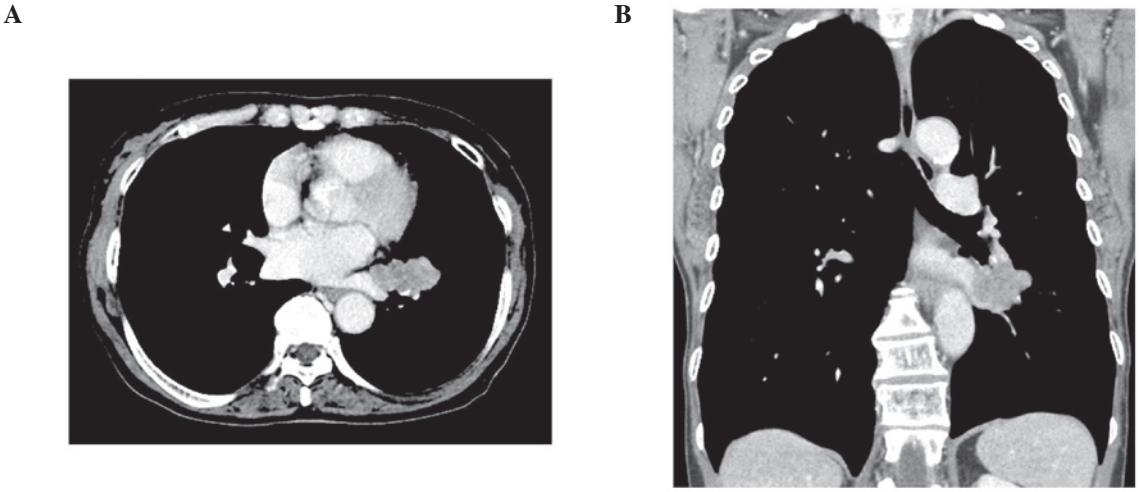

Figure 1. Computed tomography findings with contrast enhancement. (A) Axial view demonstrates a lobulated tumor with a mild heterogeneous enhancement with multifocal non-enhanced areas. The proximal bronchovascular bundle near the left hilum is involved. (B) Coronal view demonstrates the tumor occlusion of the left B8 bronchus of the lung. As presented in the axial view, the contrast enhancement is relatively mild compared with other structures.

Figure 2. Cut surface of the surgical specimen in proximity to the coronal view of the computed tomography scan. A solid, white-ish tumor with lobulated appearance is visible, with no evidence of capsule formation. It obstructs the left B8 bronchus of the lung. The border of the tumor is circumscribed, and no pulmonary parenchyma infiltration is observed on this cut surface.

myoepithelial overgrowth into a myoepithelial carcinomatous proliferation and exhibits HGT-like features.

Case report

In February 2014, a 72-year-old woman was admitted to Fujieda Municipal General Hospital (Fujieda, Shizuoka, Japan) for evaluation of a mass detected on a chest radiograph during a routine health examination. The patient had no history of smoking and her past medical history was unremarkable. Subsequent enhanced computed tomography demonstrated an enhancing lobular mass measuring 34x42x30 mm in size, with multiple focal areas of low attenuation in the S8 segment of the left lung (Fig. 1A). The proximal bronchovascular bundle adjacent to the left hilum was involved by the mass. In the coronal view, the left B8 segment of the lung was observed to be occluded by the tumor (Fig. 1B). No mediastinal lymph node metastasis or other organ metastases were observed. No abnormalities were observed in the salivary glands. A transbronchial lung biopsy of the area was conducted, and the tissue was demonstrated to contain atypical cells that were not observed in normal bronchopulmonary tissue. The serum levels of the tumor markers were as follows, with reference ranges in brackets: Carcinoembryonic antigen, 3.4 ng/ml (0-5.0 ng/ml); carbohydrate antigen 19-9, 9.1 U/ml (0-37 U/ml); squamous cell carcinoma antigen, 0.3 ng/ml (0-1.5 ng/ml); cytokeratin 19 fragment, 1.7 U/ml (0-3.5 U/ml); and pro-gastrin-releasing peptide, 87.9 pg/ml (0-80.0 pg/ml). Video-assisted thoracoscopic left lower pneumonectomy was performed. Although a definitive diagnosis of the tumor was not possible during intraoperative examination due to unfamiliar histology, gross observation of the resected tissue strongly indicated malignancy. Consequently, a lymph node dissection was performed at N2a-1, and no lymph node metastasis was identified. No recurrence has been observed for 4 months.

The surgically resected specimen was fixed with 10% buffered formalin (Formaldehyde Solution; Wako Pure Chemical Industries, Ltd., Osaka, Japan) for ~24 h. Then, 5-mm thick tissue slices were embedded in paraffin to prepare paraffin blocks. Sections (2.5-μm thick) were cut from each paraffin block for hematoxylin and eosin staining (New Hematoxylin Type G and Eosin Y; Muto Pure Chemicals Co., Ltd., Tokyo, Japan); 4-μm sections were used for immunohistochemistry (IHC). A Bench-Mark XT automated slide stainer (Ventana Medical Systems, Tucson, AZ, USA) was used to perform IHC. The primary antibodies used in the IHC analysis are listed in Table I. The ultraView Universal DAB Detection Kit (Ventana Medical Systems) was used for visualization.

Macroscopically, the tumor was solid and white-ish in color; it measured ~38x30 mm on the cut surface, which was lobulated and well-delineated without a capsule (Fig. 2). No necrotic and hemorrhagic foci were observed.

Table I. Antibodies used in the present study.

Antibody	Clone	Dilution	Catalogue no.	Antigen retrieval	Manufacturer
AE1/AE3	AE1 and AE3	1:100	AE1/ AE3-L-CE	HIER	Novocastra Laboratories, Newcastle upon Tyne, UK
αSMA	αsm-1	1:50	SMA-CE	None	Novocastra Laboratories, Newcastle upon Tyne, UK
p63	7JUL	1:100	P63-L-CE	HIER	Novocastra Laboratories, Newcastle upon Tyne, UK
p53	DO-7	Prediluted	760-2542	HIER	Ventana Medical Systems, Tucson, Arizona, USA
Ki-67	MIB-1	1:100	IR626/IS626	HIER	Dako, Glostrup, Denmark
Cyclin D1	SP4-R	Prediluted	790-4508	HIER	Ventana Medical Systems, Tucson, Arizona, USA

HIER, heat-induced epitope retrieval; SMA, smooth muscle actin.

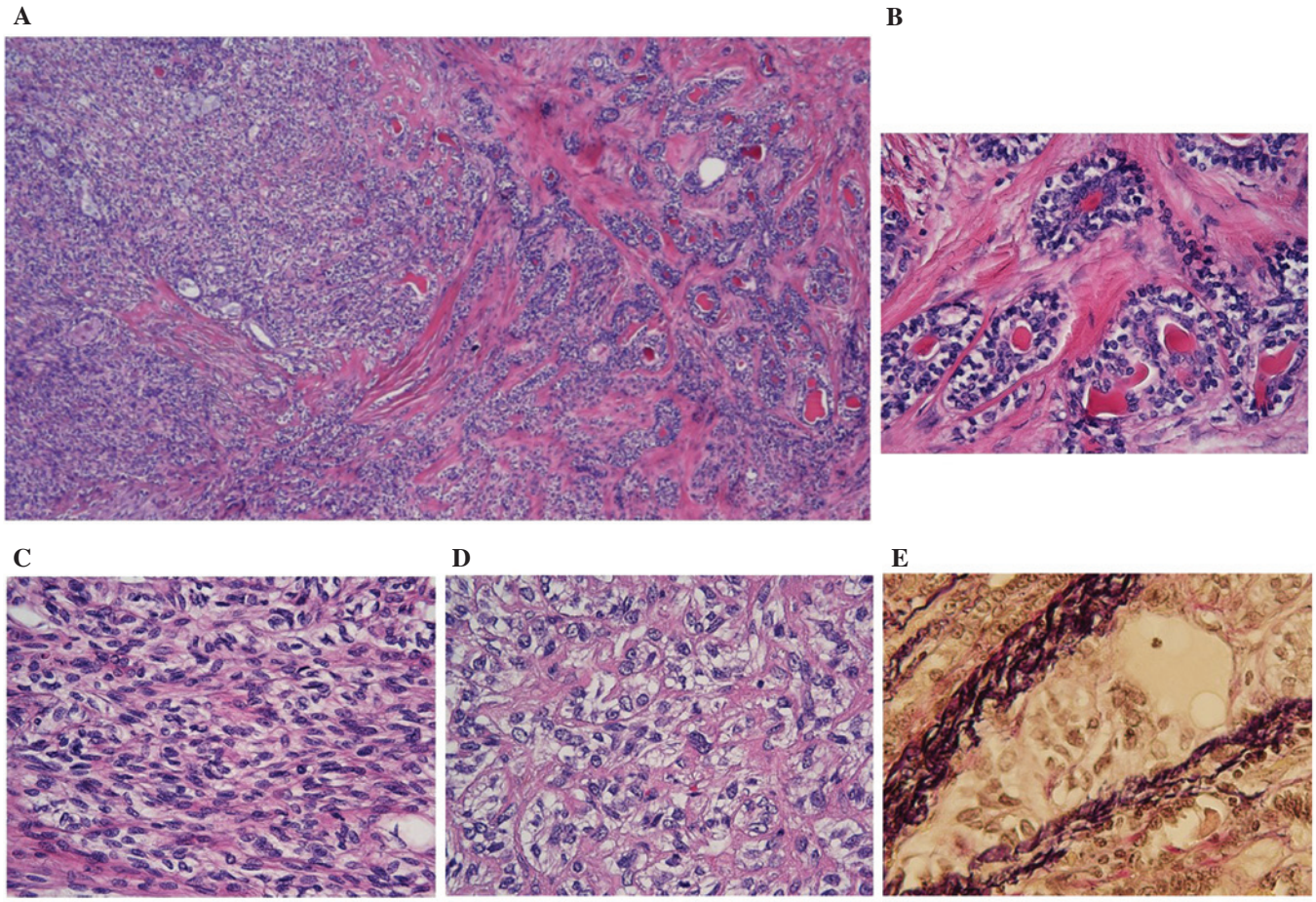

Figure 3. Microscopic findings with (A-D) hematoxylin and eosin stain and (E) Elastica van Gieson stain. (A) Low-power view (magnification, x40) of the tumor. In this field, two different components are depicted: The duct-forming component to the right of the field and the homogenous overgrowth in the admixture of spindle to polygonal tumor cells, visible from the center to the left of the field. (B) High-power view (magnification, x400) of the duct-forming component; comprising inner glandular cells with eosinophilic cytoplasm, and outer multilayered polygonal cells with clear cytoplasm. Minimal cellular atypia is visible.(C) The area with relatively monotonous proliferation of the admixture of spindle to polygonal cells possesses clear to weakly eosinophilic cytoplasm. Slight cellular atypia is visible (magnification, x400) . (D) The relatively pleomorphic component, composed of polygonal cells with nuclear atypia and clear cytoplasm (magnification, x400). (E) Venous invasion outside the circumscription of the tumor is observed. The tumor cells demonstrate increased pleomorphism inside the vein (magnification, x400).

Histopathological examination at low-power magnification (Olympus BX 51; Olympus Corporation, Tokyo, Japan) demonstrated relatively homogenous cellular proliferation overall, with differences in scattered areas (Fig. 3A). Closer visual assessment demonstrated the presence of a focal bilayered ductal component (10% of tumoral tissue; Fig. 3B), which was

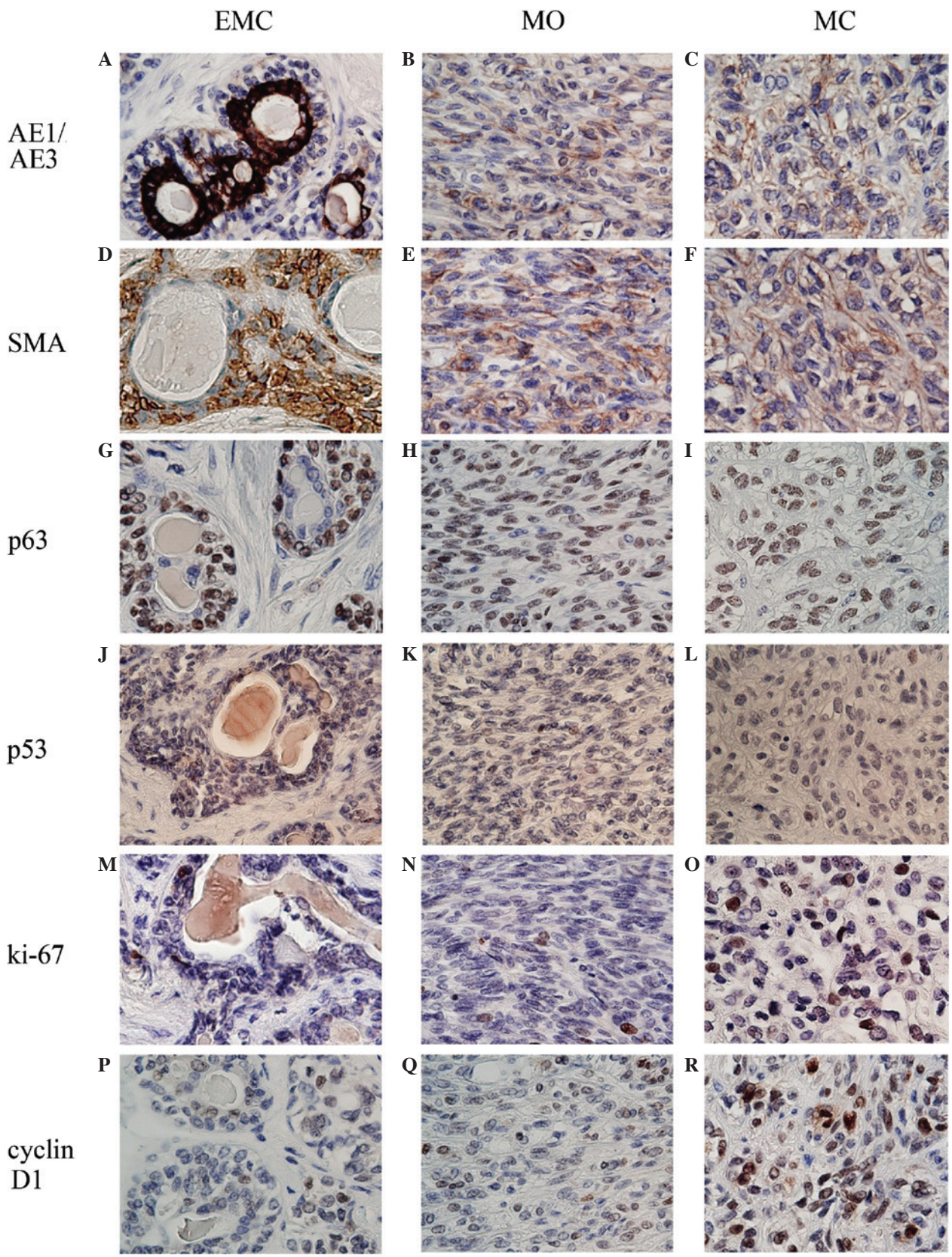

Figure 4. Immunohistochemical findings at 400X magnification. (A-C) Immunopositivity for AE1/AE3. Glandular cells in (A) EMC demonstrate strongly positive immunoreactivity for AE1/AE3. (D-F) Immunoreactivity for αSMA. Glandular cells in (D) EMC demonstrate negative immunoreactivity for αSMA. (G-I) Immunostaining for p63. In each component, the majority of the cells are positive for p63 with the exception of (G) the glandular cells in MO. (J-L) Immunostaining for p53. Accumulation of p53 in the nuclei is sparse, and no significant variations are demonstrated between the three components. (M-O) Immunostaining for Ki-67. In (M) EMC and (N) MO, a few cells are labeled with Ki-67. Labeling indexes of the former and the latter component are 1.6 and 2.8%, respectively. In (O) MC, the index is high, correlating with higher nuclear atypia (14.2%). When counting the cells, other fields were included. (P-R) Immunostaining for cyclin D1. Cyclin D1-stained cells are scattered with weak intensity in (P) EMC and (Q) MO. In (R) MC, scattered, intensely positive cells are observed, indicating overexpression of cyclin D1. EMC, epithelial-myoepithelial component; MO, myoepithelial overgrowth; MC, myoepithelial carcinoma.

overwhelmed by admixed spindle-shaped and polygonal-shaped cell components presenting with clear to weakly eosinophilic cytoplasm (70% of tumoral tissue; Fig. 3C). The remainder of the tumor mass consisted of relatively pleomorphic polygonal cells with increased nuclear atypia and clear cytoplasm situated at the advancing edge of the tumor (20% of tumoral tissue; Fig. 3D). The latter two components demonstrated a reciprocal gradual transition. The ductal structure was composed of an inner layer of glandular cells with eosinophilic cytoplasm, and an outer multilayer of polygonal cells with clear cytoplasm. Cells within the substructures demonstrated mild nuclear atypia; no mitotic cells were observed. The majority of the tumor cells did not present with increased nuclear atypia and mitotic cells were not easily detectable (<1/10 high-power fields), with the exception of a noteworthy component, 20% of which was somewhat pleomorphic and contained a few mitotic cells (≤3/10 high-power fields); indicating that this component was a higher grade. The tumor infiltrated the pulmonary parenchyma at multiple sites, irrespective of the degree of its cellular atypia. Venous invasion was demonstrated in the higher-grade component beyond the line of circumscription of the tumor (Fig. 3E). True perineural invasion was not apparent, although peripheral nerves were involved in the tumor-infiltrative area, and destructive invasion of the nerves was observed. No necrosis was observed.

IHC analyses are presented in Fig. 4: The inner cells of the ductal structure were strongly positive for AE1/AE3, while the outer cells were largely negative (Fig. 4A). By contrast, a positive reaction for α-smooth muscle actin (αSMA) and p63 was evident in the outer cells (Fig. 4D and G). This component was regarded to comprise epithelial-myoepithelial biphasic nests. The overwhelming component in the admixture of spindle and polygonal cells was weakly positive for AE1/AE3 and αSMA (Fig. 4B and E), but demonstrated a relatively strong reaction for p63 (Fig. 4H); thus, it was established to be an overgrowth of myoepithelial cells. The higher-grade component was observed to be weakly immunoreactive for AE1/AE3 and αSMA (Fig. 4C and F); however, as it maintained p63 reactivity (Fig. 4I), this component was established to be a myoepithelial carcinoma.

In order to predict biological behavior, each component of the tumor was evaluated histopathologically by using several antibodies. As a tumor marker, the tumor suppressor p53 was not densely accumulated in the nuclei and few cells displayed positive staining (Fig. 4J-L). The accumulation profiles did not vary markedly among the three components. To observe the proliferative activity of the tumor, Ki-67 was selected, and labeling indexes were calculated for the 3 components. A noticeable difference was observed; per 1,000 cells of the epithelial-myoepithelial component, myoepithelial overgrowth and myoepithelial carcinoma, the indices were 1.6, 2.8 and 14.2%, respectively (Fig. 4M-O). Overexpression of cyclin D1, one of the factors associated with cell cycle control, was not evident in the epithelial-myoepithelial or myoepithelial overgrowth components (Fig. 4P and Q); however, it was apparent in the myoepithelial carcinoma component (Fig. 4R).

Considering all the results, a diagnosis of EMC, demonstrating progression of a myoepithelial overgrowth to a myoepithelial carcinoma with higher-grade status was rendered. The surgical margins were tumor-free.

Discussion

Based on the morphological analysis, the present case conformed to the well-established observation of HGT in salivary gland carcinomas; in this case, the pulmonary EMC demonstrated progression to a higher-grade myoepithelial carcinoma via myoepithelial overgrowth (11). In addition, the present study aimed to resolve the criteria for HGT in terms of immunohistochemical characteristics. As a marker, Ki-67 is frequently used in salivary gland tumors to distinguish HGT lesions from pre-existing components (12). The previously reported Ki-67 labeling index for salivary gland EMCs ranged from <1-12% (14). The Ki-67 labeling index in the higher-grade component in the present case was 14.2%, a value that exceeds the acceptable range for a low-grade lesion, as the salivary EMC is low grade (5). There have been a number of reports that attempted to digitize the labeling index of Ki-67 in the HGT area of an EMC, and one case documented that the Ki-67 labeling index of the HGT area in a salivary EMC was 40% (for a review, see reference 15). A detailed image demonstrating Ki-67 immunostaining was presented in another study on salivary EMC; although the value of the labeling index was not mentioned (10), it was estimated to be higher compared with the index in the present case. Therefore, the higher-grade component in the present case cannot be categorized as an HGT; another term, HGT-like, is better applied to the present case. This designation is well-defined in terms of the malignant range of salivary EMCs. It falls within the range of intermediate- to high-grade malignancy (10). Thus, for the present study, progression from a low-grade to an intermediate-grade malignancy is defined as HGT-like.

Other markers used to define HGT are p53 and cyclin D1. In the majority of salivary gland tumor types, the p53 staining is stronger in the HGT component compared with the pre-existing component (12). Unlike conventional HGT, in the present case, $p53^+$ cells were scattered throughout the tumor, with no recognizable variability. However, previous studies have also described negative staining in acinic cell carcinomas (16,17). These inconsistencies indicate that p53 alteration is not the primary mechanism for HGT.

Cyclin D1 is highly expressed in HGT of salivary gland tumors (12) and was overexpressed at the HGT-like site in the present case. This indicates the stepwise progression from the pre-existing tumor, in a pathway similar to that in HGT in salivary gland tumors. Cyclin D1 is established to induce chromosomal instability (18); it is recruited to DNA via sequence-specific binding proteins and leads to differential gene expression of chromatin reorganizing proteins (19). This abnormal mitotic regulation can result in increased aneuploidy, in addition to structural chromosomal aberrations, including translocation and duplications (19). This molecular basis provides a plausible explanation to the hypothesis that increased cyclin D1 expression resulted in the HGT-like histological features of the tumor in the present case.

A significant correlation between the size of the EMC and the occurrence of HGT in salivary glands has been documented (20). A range of 2-11 cm (mean, 6.3 cm) was reported in 17 cases of salivary EMC demonstrating HGT. Pulmonary salivary gland-type tumors are detected earlier since patients experience discomfort due to the tumor's proximity with the

bronchial tree (3); thus, the tumor size was smaller in these cases, ranging between 1.3 and 4.0 cm (mean, 2.5 cm) in 7 cases of pulmonary EMC (2). In addition, several previous studies have described the size of pulmonary EMCs: The size in the majority of these cases was smaller than the mean size for EMCs with HGT, as described above (3). This observation may explain why definite HGTs have not been detected in pulmonary EMCs.

Pathological features corresponding to HGT were traditionally termed 'dedifferentiation'; this term applied solely to high-grade neoplasms, which had progressed from low-grade neoplasms and had lost all the histological characteristics of their original lineage (10). More recently, it has been identified that neoplasms maintaining their original lineage also demonstrate significant malignancy. Previous studies have identified EMCs with two types of HGT as follows: i) Those that lack myoepithelial features (20,21); and ii) those that maintain myoepithelial characteristics with a certain degree of nuclear atypia (11,21). The latter are also termed EMCs with myoepithelial anaplasia. The high-grade area in the latter often develops from a gradual transition from myoepithelial overgrowth in the low-grade EMC area (11,15,20). The tumor in the present case exhibited weak, but evidently positive staining of αSMA in the HGT-like component, similar to the staining observed in EMCs with myoepithelial anaplasia (11,21).

HGT occurs as three forms in EMCs of salivary glands. Of the 22 cases investigated by Baker *et al* (13) HGT was demonstrated in the epithelial component in 10 cases (45.5%), in the myoepithelial component in 2 cases (9.1%), and in both of these components in 3 cases (13.6%), with the remaining 7 cases not clearly defined. The present case possessed an HGT-like component originating from the myoepithelial part, corresponding to the second most frequent form of the three.

In the present case, metastasis to nodes and distal organs was not observed and the clinical outcome of the patient is good at present. Since this outcome contradicts the highly malignant character of HGT, the use of the term 'HGT-like' is verified from the clinical point of view (21). However, venous invasion and myoepithelial anaplasia, which are 2 of the 4 significant predictors of reduced disease-free survival in EMCs of the salivary glands (positive margin status, necrosis, angiolymphatic invasion and myoepithelial anaplasia), were present in the current case (11). EMCs of the salivary gland have a local recurrence rate of 23-80% and a rate of metastasis of 14-25% (11), with long intervals between recurrence (mean, 5 years) and metastasis (mean, 15 years) (22,23). These data indicate the possibility of a poor outcome in the form of recurrence and/or metastasis to distant organs in the future. A thorough follow-up, including the examination of distant organs for signs of metastasis, is required for this patient.

The present case identified a pulmonary EMC demonstrating progression from a myoepithelial overgrowth to a myoepithelial carcinoma (with an HGT-like component). Morphological and immunohistochemical status, particularly overexpression of cyclin D1 and its possible molecular functions, indicated a stepwise progression towards a higher grade of malignancy; the present case appeared to follow a similar pathway towards HGT as is observed in salivary gland-type tumors. Although the Ki-67 labeling index in the HGT-like component did not reach the value reported previously in other salivary EMCs, cyclin D1 was overexpressed exclusively in the HGT-like component of the tumor. To the best of our knowledge, this is the first report of pulmonary EMC described with a thorough investigation of the potential HGT-associated molecular mechanisms. Additional studies with more subjects enrolled are required to elucidate the nature of pulmonary EMC and the clinicopathological importance of an HGT and/or HGT-like status.

References

1. Kang DY, Yoon YS, Kim HK, *et al*: Primary salivary gland-type lung cancer: surgical outcomes. Lung Cancer 72: 250-254, 2011.
2. Zhu F, Liu Z, Hou Y, *et al*: Primary salivary gland-type lung cancer: clinicopathological analysis of 88 cases from China. J Thorac Oncol 8: 1578-1584, 2013.
3. Song DH, Choi IH, Ha SY, *et al*: Epithelial-myoepthelial carcinoma of the tracheobronchial tree: the prognostic role of myoepithelial cells. Lung Cancer 83: 416-419, 2014.
4. Donath K, Seifert G and Schmitz R: Diagnosis and ultrastructure of the tubular carcinoma of salivary gland ducts. Epithelial-myoepithelial carcinoma of the intercalated ducts. Virchows Arch A Pathol Pathol Anat 356: 16-31, 1972 (In German).
5. Fonseca I and Soares J: Epithelial-myoepithelial carcinoma. In: World Health Organization Classification of Tumours: Pathology and Genetics of Head and Neck Tumours. Barnes L, Eveson JW, Reichart P and Sidransky D (eds). 3rd edition. IARC Press, Lyon, France, pp225-226, 2005.
6. Corio RL, Sciubba JJ, Brannon RB and Batsakis JG: Epithelial-myoepithelial carcinoma of intercalated duct origin. A clinicopathologic and ultrastructural assessment of sixteen cases. Oral Surg Oral Med Oral Pathol 53: 280-287, 1982.
7. Moran CA: Primary salivary gland-type tumors of the lung. Semin Diagn Pathol 12: 106-122, 1995.
8. Pelosi G, Fraggetta F, Maffini F, Solli P, Cavallon A and Viale G: Pulmonary epithelial-myoepithelial tumor of unproven malignant potential: report of a case and review of the literature. Mod Pathol 14: 521-526, 2001.
9. Nguyen CV, Suster S and Moran CA: Pulmonary epithelial-myoepithelial carcinoma: a clinicopathologic and immunohistochemical study of 5 cases. Hum Pathol 40: 366-373, 2009.
10. Nagao T: "Dedifferentiation" and high-grade transformation in salivary gland carcinomas. Head Neck Pathol 7 (Suppl 1): S37-S47, 2013.
11. Seethala RR, Barnes EL and Hunt JL: Epithelial-myoepithelial carcinoma: a review of the clinicopathologic spectrum and immunophenotypic characteristics in 61 tumors of the salivary glands and upper aerodigestive tract. Am J Surg Pathol 31: 44-57, 2007.
12. Costa AF, Altemani A and Hermsen M: Current concepts on dedifferentiation/high-grade transformation in salivary gland tumors. Patholog Res Int 2011: 325965, 2011.
13. Baker AR, Ohanessian SE, Adil E, Crist HS, Goldenberg D and Mani H: Dedifferentiated epithelial-myoepithelial carcinoma: analysis of a rare entity based on a case report and literature review. Int J Surg Pathol 21: 514-519, 2013.
14. Arif F, Wu S, Andaz S and Fox S: Primary epithelial myoepithelial carcinoma of lung, reporting of a rare entity, its molecular histogenesis and review of the literature. Rep pathol 2012: 319434, 2012.
15. Yang S and Chen X: Epithelial-myoepithelial carcinoma with high grade transformation. Int J Oral Maxillofac Surg 41: 810-813, 2012.
16. Henley JD, Geary WA, Jackson CL, Wu CD and Gnepp DR: Dedifferentiated acinic cell carcinoma of the parotid gland: A distinct rarely described entity. Hum Pathol 28: 869-873, 1997.
17. Di Palma S, Corletto V, Lavarino C, Birindelli S and Pilotti S: Unilateral aneuploid dedifferentiated acinic cell carcinoma associated with bilateral-low grade diploid acinic cell carcinoma of the parotid gland. Virchows Arch 434: 361-365, 1999.
18. Casimiro MC and Pestell RG: Cyclin d1 induces chromosomal instability. Oncotarget 3: 224-225, 2012.
19. Casimiro MC, Crosariol M, Loro E, *et al*: ChIP sequencing of cyclin D1 reveals a transcriptional role in chromosomal instability in mice. J Clin Invest 122: 833-843, 2012.
20. Roy P, Bullock MJ, Perez-Ordoñez B, Dardick I and Weinreb I: Epithelial-myoepithelial carcinoma with high grade transformation. Am J Surg Pathol 34: 1258-1265, 2010.
21. Cheuk W and Chan JK: Advances in salivary gland pathology. Histopathology 51: 1-20, 2007.

22. Cho KJ, el-Naggar AK, Ordonez NG, Luna MA, Austin J and Batsakis JG: Epithelial-myoepithelial carcinoma of salivary glands. A clinicopathologic, DNA flow cytometric, and immunohistochemical study of Ki-67 and HER-2/neu oncogene. Am J Clin Pathol 103: 432-437, 1995.

23. Luna MA, Ordonez NG, Mackay B, Batsakis JG and Guillamondegui O: Salivary epithelial-myoepithelial carcinomas of intercalated ducts: a clinical, electron microscopic, and immunocytochemical study. Oral Surg Oral Med Oral Pathol 59: 482-490, 1985.